

Microscopic Origin of the Fast Blue-Green Luminescence of Chemically Synthesized Non-oxidized Silicon Quantum Dots

Kateřina Dohnalová,* Anna Fučíková, Chinnaswamy P. Umesh, Jana Humpolíčková, Jos M. J. Paulusse, Jan Valenta, Han Zuilhof, Martin Hof, and Tom Gregorkiewicz

The microscopic origin of the bright nanosecond blue-green photoluminescence (PL), frequently reported for synthesized organically terminated Si quantum dots (Si-QDs), has not been fully resolved, hampering potential applications of this interesting material. Here a comprehensive study of the PL from alkyl-terminated Si-QDs of 2–3 nm size, prepared by wet chemical synthesis is reported. Results obtained on the ensemble and those from the single nano-object level are compared, and they provide conclusive evidence that efficient and tunable emission arises due to radiative recombination of electron–hole pairs confined in the Si-QDs. This understanding paves the way towards applications of chemical synthesis for the development of Si-QDs with tunable sizes and bandgaps.

1. Introduction

Silicon quantum dots (Si-QDs) with bright and spectrally tunable photoluminescence (PL) could constitute a benign

alternative to toxic, rare, and/or expensive semiconductor QDs, which are used nowadays in optoelectronics, photonics, photovoltaics, and bio-imaging. However, i) the most studied PL from oxidized Si-QDs has very low radiative rates and is not spectrally tunable and ii) the best understood H-terminated Si-QDs with spectrally tunable PL also exhibit low radiative rates and are chemically unstable.^[1–4] Presently, the most promising candidates for bright silicon-based tunable emitters are Si-QDs capped with organic molecules such as alkyl chains. These materials i) can be synthesized in macroscopic yields from the gas^[5–8] and liquid phases (supercritical fluids,^[9–11] micro-emulsion synthesis,^[12–16] and via reduction–oxidation processes^[17–22]); ii) have stable surface passivation due to the strong covalent Si–C bond, which is resistant to oxidation; iii) do not aggregate;^[9,15] iv) allow for versatile (bio-) functionalization;^[22,23] v) are nontoxic;^[23,24] and vi) exhibit bright photo-stable blue-green PL with fast decay.^[14,15,25–27] This PL lifetime, however, is more than three orders of magnitude faster ($\sim 10^9$ – 10^8 s^{–1}) than expected for the excitonic emission ($\sim 10^6$ – 10^5 s^{–1}).^[1,4] The situation is even more complicated, as most of the various molecules (solvents or chemical compounds), used for or produced by the synthesis procedure of these materials, show nanosecond emission in a similar spectral region, and this might overlap or even dominate the experimentally measured PL.^[28] To investigate the microscopic origin of the fast blue-green PL in organically terminated Si-QDs, we synthesize alkyl-terminated, 2–3 nm

Dr. K. Dohnalová, Prof. T. Gregorkiewicz
Van der Waals-Zeeman Institute
University of Amsterdam
Science Park 904, Amsterdam, NL-1098 XH
The Netherlands
E-mail: k.dohnalova@uva.nl



Dr. A. Fučíková, Dr. J. Valenta
Department of Chemical Physics and Optics
Faculty of Mathematics and Physics, Charles University
Ke Karlovu 3, Prague 2, CZ-12116, Czech Republic
C. P. Umesh, Dr. J. M. J. Paulusse,^[+] Prof. H. Zuilhof
Laboratory of Organic Chemistry
Wageningen University
Dreijenplein 8, Wageningen, NL - 6703 HB, The Netherlands
Dr. J. Humpolíčková, Prof. M. Hof
J. Heyrovský Institute of Physical Chemistry of the Academy of Sciences
of Czech Republic, v. v. i., Dolejškova 2155/3, Prague 8, CZ-182 23
Czech Republic

[+] Current address: MIRA Institute, Department of Biomedical Chemistry, University of Twente, Building Zuidhorst, Room ZH 116, Enschede, NL-7500 AE, The Netherlands

DOI: 10.1002/sml.201200477

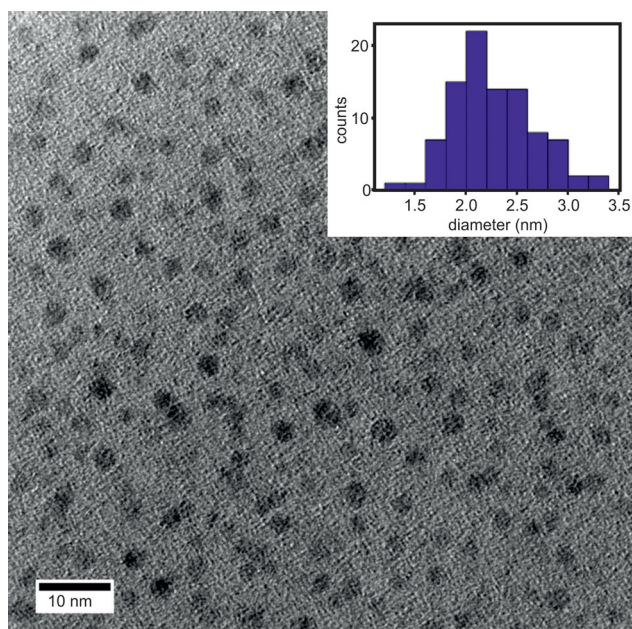


Figure 1. TEM image of butyl-capped Si-QDs with a size distribution of 2.2 ± 0.5 nm (inset).

diameter Si-QDs using wet chemistry and compare the PL of the resulting QDs at the ensemble and single-QD levels.

2. Results and Discussion

2.1. Sample Preparation

Si-QDs terminated by *n*-butyl were prepared via a wet-chemical method^[22] adapted from Kauzlarich and co-workers.^[18] The average size of Si-QDs is $D = 2.2 \pm 0.5$ nm, as estimated by transmission electron microscopy (TEM) (**Figure 1**). NMR spectra confirm that Si-QDs were prepared un-oxidized (see Supporting Information (SI), Figure S1–S3). Full characteristics of the samples can be found in the literature.^[22] For optical spectroscopy, the free-standing Si-QDs were dispersed in UV grade ethanol. For single-QD spectroscopy, highly diluted colloids were drop-casted onto a quartz slide. Fourier Transform infrared (FTIR) spectra were collected from extensively dried colloids of Si-QDs, redispersed in CCl_4 between NaCl crystals.

2.2. Si-QD Ensemble Photoluminescence

Size-dependent PL emission of the colloidal sample under various excitation wavelengths is illustrated by the

photograph in **Figure 2a**. The ensemble absorbance, the PL spectra and PL lifetime, of the colloidal sample are plotted in Figure 2b and c, respectively. The absorbance shows spectral profile characteristic for band-to-band absorption. The PL spectra in Figure 2b were excited at three wavelengths of 320, 350, and 405 nm, indicated by arrows on the absorbance curve. The spectra are plotted normalized to the absorbance at the particular excitation wavelength (full areas) or to the peak intensity (dashed lines). In the first case, the integrated PL emission is roughly proportional to the external quantum efficiency (QE). The absolute QE under 370 nm excitation has been estimated to be $\sim 3.7\%$ (for details, see SI). Therefore, it follows that the QE under 320 nm excitation would be $< 1\%$ and at 405 nm around $\sim 11\%$. The QE increases with the size of the Si-QDs, in agreement with the previous studies of organically capped Si-QDs.^[5] This effect has been previously interpreted as a result of better passivation of the surface defects in nanoparticles with lower surface curvature.^[30] The PL spectra normalized to the peak intensity (dashed lines), show a clear spectral shift with the excitation wavelength, as a result of the size-distribution, and concomitant size-dependent optical properties (see also Figure 2a). The

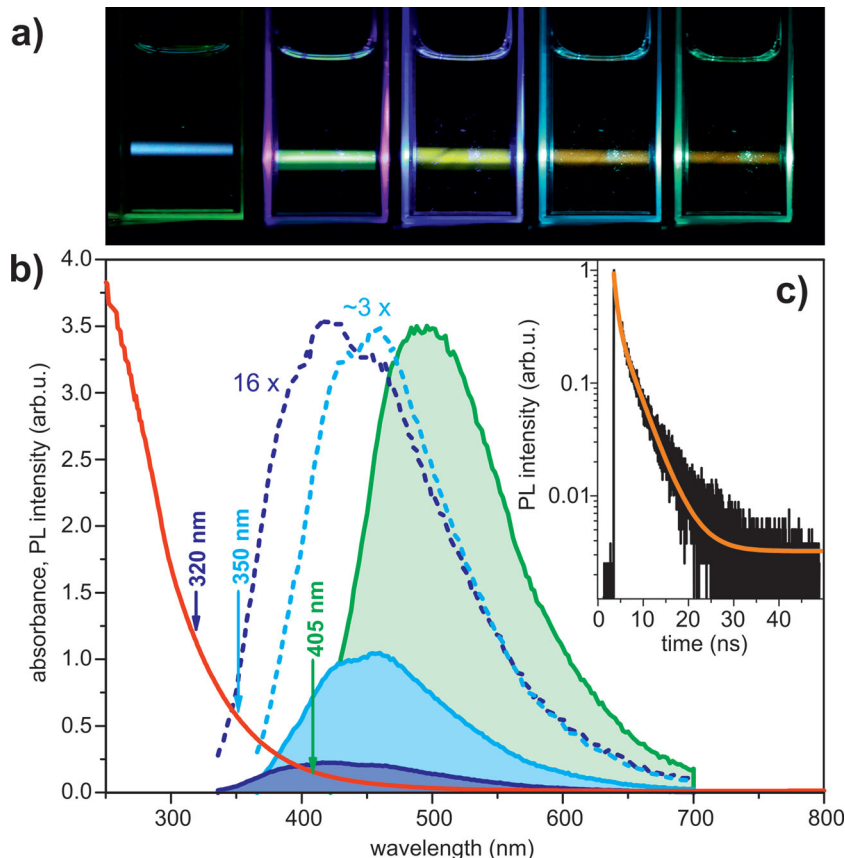


Figure 2. a) Photograph of PL of the sample under nanosecond-pulsed laser excitation with 380, 450, 465, 483, and 495 nm wavelengths (from left to right); image credit: M. T. Trinh. b) Absorbance (red) and PL spectra excited at three different wavelengths by a Xe lamp: 320 nm (dark blue), 350 nm (light blue), and 405 nm (green). The as-measured PL spectra were normalized to absorbance at the relevant excitation wavelength (full areas) and by the PL emission peak intensity (dashed lines). c) PL lifetime at 500 nm under femtosecond-pulsed laser excitation at 370 nm (instrumental response time is ~ 26 ps).

decay of PL at 500 nm is plotted in the inset of Figure 2c and features two components, with time constants of 723 ± 9 ps and 3.80 ± 0.03 ns. This is in good agreement with the PL lifetime observed in the past for organically terminated Si-QD samples.^[10,14,15,27,31] Such a fast decay cannot be explained by existing models of excitonic emission in Si-QDs. It has been suggested in the past that the fast blue-green emission might occur as a result of Γ - Γ recombination.^[27] However, due to efficient competition with carrier cooling, this emission should be accompanied by the slow (approximately microsecond decay) red PL from the band-to-band Γ -X transitions,^[32] which is not observed (Figure 2b). Further, a very spectrally similar blue nanosecond band in oxidized Si-QDs has been assigned to oxygen-related defect states^[33] or ultra-small clusters.^[34] This possibility we exclude here by comparison of the PL spectra for the as-synthesized and oxidized samples (Figure S4, SI). Moreover, similar PL with fast decay has been observed independently of the preparation technique and the type of C-linked surface ligands used,^[25,26] which suggests intrinsic excitonic origin. This is supported by the ab initio simulations for the UV-emitting ultra-small alkyl-terminated Si clusters,^[35] which predict an excitonic origin for PL and negligible influence of surface ligands on the optical bandgap. This theoretical modeling, however, does not explain the fast radiative rate and does not give any information on the spectral tunability of PL from larger Si-QDs, potentially emitting in the visible range and interesting for applications. In the present case, to confirm an intrinsic excitonic and exclude an extrinsic (defect or impurity-related) origin of PL, we have conducted a series of single-QD spectroscopy measurements of PL spectra and established the lifetime of single Si-QDs.

2.3. Single Si-QD Photoluminescence

Single Si-QD PL spectra reported in the literature were acquired from red-emitting Si-QD samples—from large organically terminated Si-QDs with nanosecond PL lifetime,^[10,31] or oxidized Si-QDs with microsecond PL lifetime.^[36–40] On the other hand, to the best of our knowledge, a single-QD spectroscopy study has not yet been performed for small blue-green-emitting Si-QDs synthesized using wet chemistry. Also the nanosecond lifetime reported in the past in single-QD spectroscopy studies were obtained from red-emitting ensembles^[10] and not for a single alkyl-terminated Si-QD.

In **Figure 3** we show single Si-QD PL spectra measured in the wide-field microscopy regime and the PL lifetime of

individual QDs in the confocal regime (Figure 3a). A typical PL decay for a single Si-QD is shown in Figure 3c. A bi-exponential decay function with parameters identical to those measured for the ensemble in Figure 2c (orange curve), convoluted with the measured instrumental response function of the detector, gives an excellent fit to the acquired data (black curve). This confirms the common origin of the PL from both single Si-QDs and Si-QD ensembles.

Single Si-QD spectra are known to show characteristic phonon replicas, occurring as a result of enhanced electron-phonon coupling, which causes dissipation of the recombination energy into vibration modes. This has been concluded in the past for oxidized^[36–40] as well as organically capped^[10,31] Si-QDs. In this study, we captured in total 1000 PL spectra of the randomly chosen single Si-QDs. Out of these, 233 exhibited well-defined structure, which we assigned to phonon replicas. The energy of the involved phonon is found to be on average ~ 167 meV (Figure 3d). While in bulk crystalline Si, phonon replicas are usually related to vibrations of the crystalline matrix, in small Si-QDs, due to the enhanced

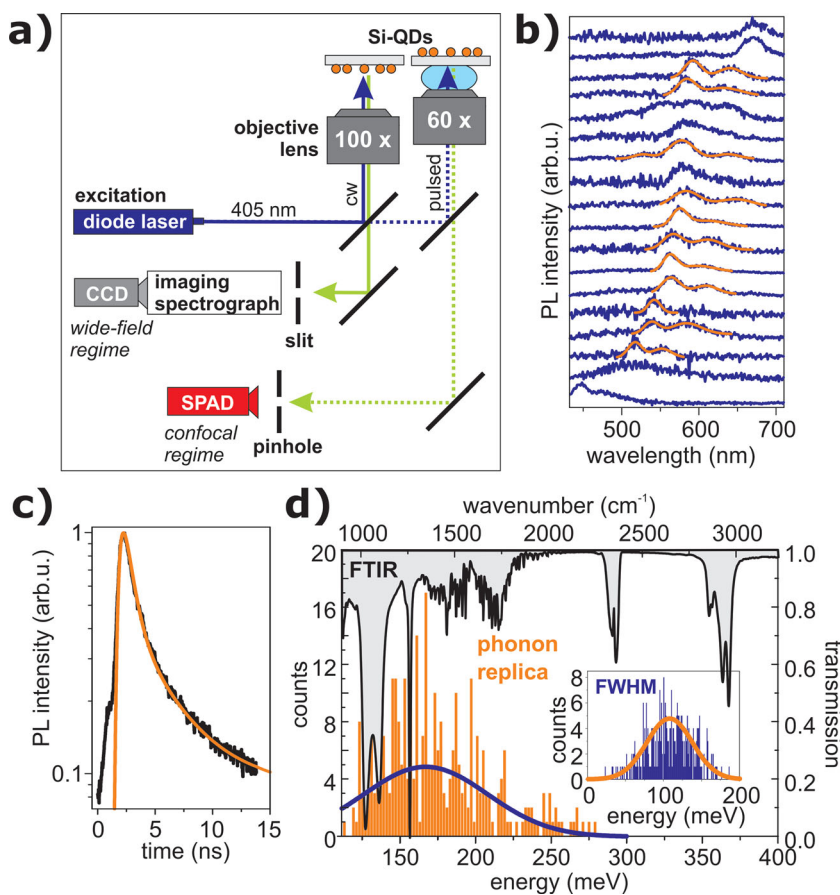


Figure 3. a) Schematic sketch of the single-QD spectroscopy setup in wide-field and confocal regimes. b) Single Si-QD PL spectra, between 450 and 700 nm. Spectra are normalized and shifted along y-axis. c) Single Si-QD PL lifetime, excited by a picosecond-laser pulse at 405 nm. Signal was detected in a confocal regime microscopy setup (instrumental response time is ~ 600 ps). d) FTIR transmission spectrum (black line) compared with histogram of phonon energy (orange bars) evaluated from structured single Si-QD PL spectra. Distribution is close to normal; therefore the histogram is fitted with a Gaussian function (blue line). Inset: Histogram of phonon replica's FWHM, with normal distribution, fitted with Gaussian function (orange line).

influence of the surface, phonon replicas predominantly arise due to coupling with surface vibrations, usually of higher energies. This is also observed in the present study. To identify the involved surface phonon, we compare the replica energy with the FTIR spectrum of the sample (Figure 3d). The maximum of the histogram coincides with the Si–C stretching vibrational mode at 1260 cm^{-1} . The appearance of this peak, together with the scissoring Si–C mode at 1459 cm^{-1} , confirms covalent bonding with C on the Si-QD surface. Other strong absorption peaks correspond to symmetric and asymmetric CH_2 stretching (2873 and 2931 cm^{-1}), asymmetric CH_3 stretching (2960 cm^{-1}), and CH_2 rocking or wagging (1024 cm^{-1}) vibrational modes. The signal at 1070 cm^{-1} can be assigned to Si–O–Si or Si–O–C vibrations (occurring due to inevitable oxidation, which occurs due to the sample treatment involved in FTIR spectroscopy); however, its negligible role in PL (Figure 3d) indicates that the major part of the investigated Si-QDs are not oxidized. This is further supported by the absence of red PL, which is characteristic of oxidized Si-QDs (Figure S4, SI).

The average full width at half maximum (FWHM) of the PL bands is $\sim 110\text{ meV}$ (inset in Figure 3d), in agreement with previous findings for Si-QDs.^[31,36–38] Such a large line-width was previously explained as being due to the participation of one or more Si phonons in the light emission process.^[40] However, this explanation does not apply for organically capped Si-QDs, as the nanosecond decay time indicates a phononless recombination. Therefore the line broadening is more likely to occur due to the fluctuating properties of the environment at room temperature. Values of the phonon energy and FWHM follow a normal distribution (fitted with a Gaussian function in Figure 3d) and are both rather broad—the standard deviation of replica energies and FWHM is 41 and 30 meV, respectively. This broadening is largely influenced by the size distribution. This is apparent from **Figure 4a** and **b**, where the spectral dependence of both parameters is plotted. Both the phonon energy and FWHM exhibit a slight linear increase with reduced average Si-QD size, i.e., with increasing emission energy, which has also been observed before for well-defined oxidized Si-QDs.^[38] The size dependence of the phonon energy could appear as a result of varying contributions of the different vibration modes of the core and surface bonds with changing surface-to-volume ratio. Also the average energetic distance between the electronic states increases with reduced Si-QD size, due to the lower density of states. Therefore, the energy dissipation in smaller Si-QDs can take place exclusively with participation of

vibration modes with larger energy. In summary, we conclude that while on average the Si–C vibration mode dominates the energy dissipation mechanism, simple assignment of a single vibration mode to the replica is not possible. The replicas rather appear as a result of a statistical mixture of various surface and volume phonons, somewhat different for each Si-QD size and surface termination.

In agreement with previous observations,^[38] the strength of the electron–phonon coupling, given by the Huang–Rhys factor, S , is size-dependent (Figure 4c) and can be additionally modified for smaller Si-QDs by the polarity of the local environment.^[41] S defines an average number of vibration quanta involved in light emission in a single Si-QD. The spectrum of a single Si-QD with diameter D shows n replicas ($n = 0$ for zero-phonon line) with intensities $I(n, S(D))$ and can be fitted by a function $I(n, S(D)) = \frac{S(D)^n e^{-S(D)}}{n!}$. The spectral dependence of S in Figure 4c cannot be precisely established due to the low number of single Si-QD spectra with a higher number of phonon replicas. Nevertheless, the general trend of increasing S with reduced Si-QD size can be recognized, as indicated by the red dashed line (guide to

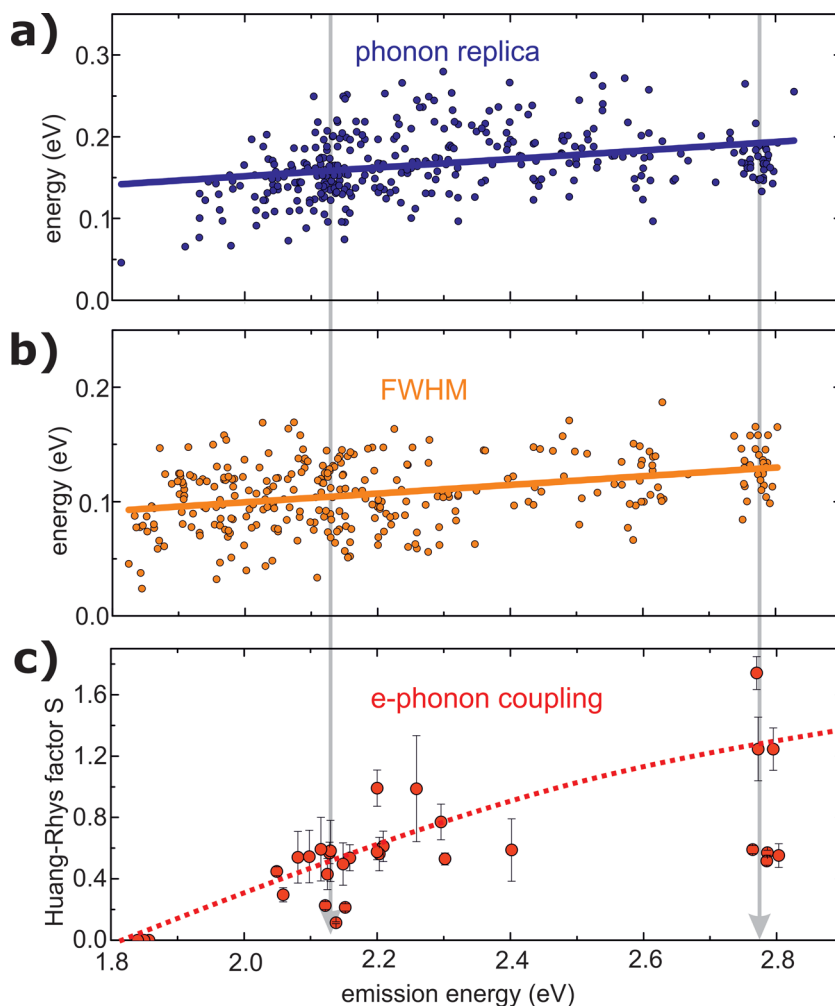


Figure 4. Spectral dependence of the a) phonon energy, b) replica's FWHM, and c) Huang–Rhys factor. Colored lines in (a,b) are linear fits and in (c) a guide to the eye. Gray arrows indicate two emission energies, at which the structured single Si-QD spectra were observed with a higher probability.

the eye). This has indeed been expected: For bulk Si, $S \approx 0$, and with size reduction of Si-QDs, S should increase proportional to D^{-3} or D^{-4} for coupling to volume or surface vibrations, respectively.^[42] We also note that additional resonant processes, such as trapping at defect states^[38] or resonance of vibration energy with some of the electronic transitions,^[43,44] can considerably enhance the Huang–Rhys factor. Such a resonant enhancement of the electron–phonon coupling might be the reason for the observed inhomogeneity of the abundance of structured single Si-QD spectra, appearing in contrast to homogeneous abundance of all single Si-QD spectra (Figure 5a). Technically, these abundances were obtained by summing up the normalized single Si-QD PL spectra. For comparison, we show also the abundance of the spectral positions of the main replica in the structured single Si-QD PL spectra (orange bars). It is clear that the structured spectra occur mainly around two emission wavelengths at 580 and 450 nm (also indicated by the gray arrows in Figure 4), in contrast to the homogeneous distribution of the non-structured spectra within the ensemble PL. This can be also seen from Figure 5b, where all of the 1000 acquired single PL spectra are plotted and normalized to the peak maxima. Similar observations have been reported for Si-QDs by other groups.^[10,31,38] Inhomogeneity in spectral occurrences of structured single Si-QD spectra might be related to a complex size-dependence of the electron–phonon coupling strength in small Si-QDs,^[38] as mentioned above, or to polaron formation, caused by a possible resonance between the electronic states and vibration energy.^[43,44] Finally, it is necessary to mention that such an inhomogeneity could also occur due to the unfortunate, but difficult to avoid, selectivity of single-QD measurements, which brings forward the most bright (and therefore better resolved) spectra, neglecting those of lower quality, which are usually in the majority. The summation of the single Si-QD spectra and the PL spectrum of Si-QD ensembles, both excited by a continuous wave (cw) illumination at 405 nm, are plotted in Figure 5c. For the sake of comparison, PL spectra were normalized at 600 nm, where the spectral profiles appear to be identical. This agreement indicates that single Si-QDs are photostable and do not oxidize under heavy UV illumination by a highly focused

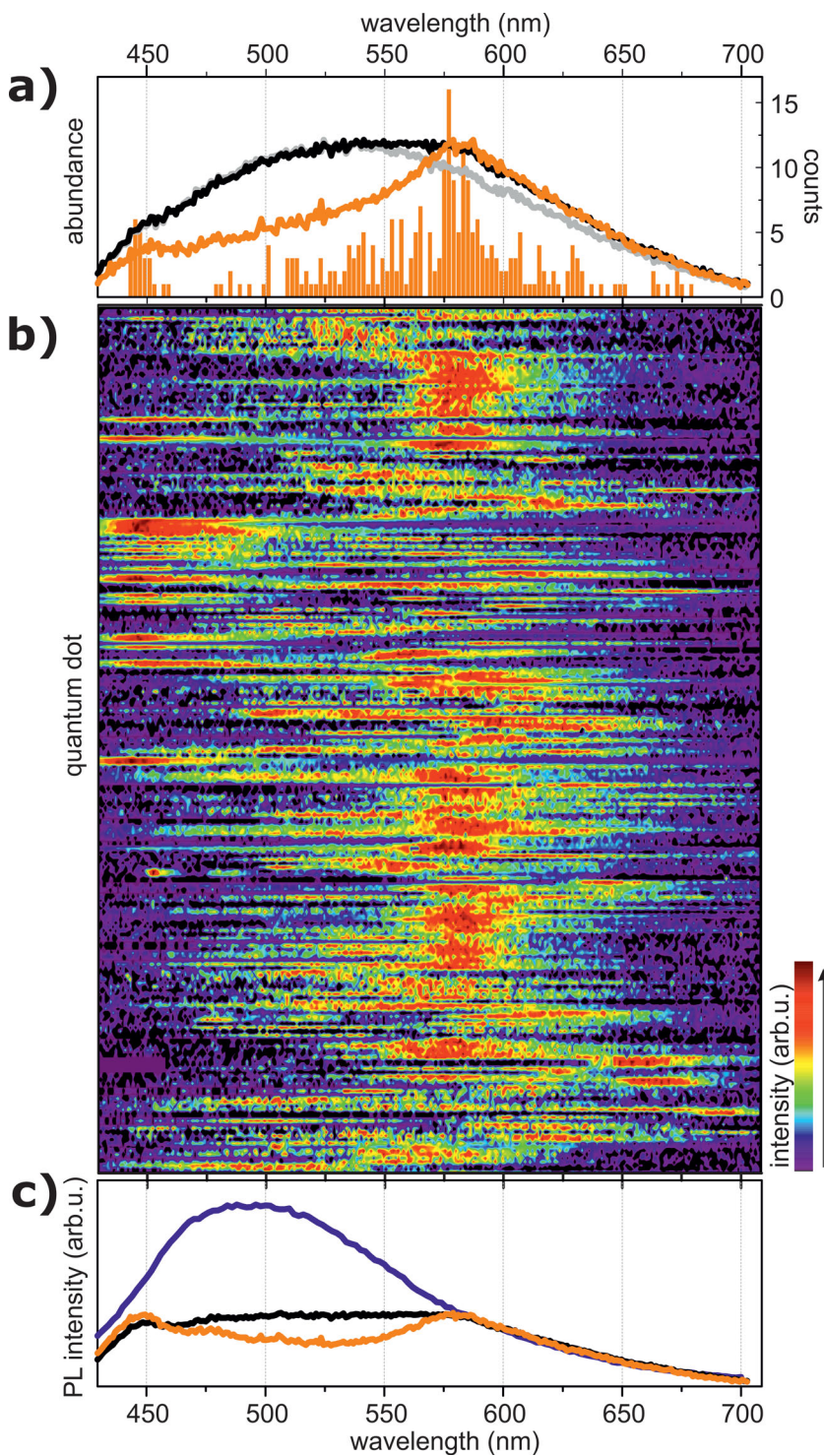


Figure 5. a) Abundances of the single Si-QD PL spectra: non-structured only (gray), structured only (orange), and all acquired spectra together (black). For comparison, abundance of the spectral position of the zero phonon replica is shown in the structured spectra (orange bars). b) All 1000 acquired single Si-QD PL emission spectra (normalized by peak intensity). c) Comparison of the PL emission spectra of the Si-QDs ensemble (blue) and summed single Si-QDs spectra: structured only (orange) and all spectra (black).

0.43 mW cw laser beam (the summed single Si-QD spectra do not show any significant peak at ~670 nm, where a strong PL band appears when Si-QDs are oxidized; see SI, Figure S4).

0.43 mW cw laser beam (the summed single Si-QD spectra do not show any significant peak at ~670 nm, where a strong PL band appears when Si-QDs are oxidized; see SI, Figure S4).

Similar spectral positions, lifetimes, and observation of Si-C phonon replicas confirm the common origin of the single Si-QD spectra and the ensemble blue-green PL. All the observed features provide firm evidence that emission is related to the Si-QDs themselves, rather than defects, molecular contaminants, or impurities: i) the characteristic phonon replicas, ii) their size-dependent behavior, iii) spectrally shifting single Si-QD PL spectra, and also iv) negligible bleaching during measurements, lasting over tens of minutes (see SI, Figure S5).

3. Conclusion

Ensemble PL from alkyl-terminated Si-QDs occurs in the blue-green spectral region and has a fast nanosecond lifetime. The single Si-QD spectra feature characteristic of semiconductor QDs and are clearly different from those of single molecules or defect-related emissions. Also the PL lifetime of single Si-QDs and Si-QD ensembles are identical. Furthermore, the ensemble properties are reproduced by summing up contributions of individual QDs. Upon oxidation, PL characteristics change, and become consistent to those reported in the past for oxygen-terminated Si-QDs prepared, e.g., by co-sputtering.^[29] In view of this evidence we conclude that the blue-green PL with nanosecond lifetime is truly intrinsic to Si-QDs. Our study goes beyond simple comparison of results obtained by different techniques, e.g., PL and TEM, as is common in previous investigations of chemically synthesized Si-QDs. In that way we provide an unambiguous proof that chemical synthesis is capable of yielding stable, non-oxidized and alkyl-terminated Si-QDs exhibiting bright nanosecond emission, tunable in the visible spectral region.

4. Experimental Section

Synthesis of Si-QDs: Si-QDs of average size (2–3 nm) were synthesized using wet chemistry: magnesium silicide (Mg_2Si) was oxidized with bromine (Br_2) in refluxing *n*-octane for 3 days. The formed bromine-terminated Si-QDs were capped using *n*-butyl-lithium, resulting in *n*-butyl-terminated Si-QDs. The main side-product, bromo-octane, and other impurities, were removed using silica column chromatography. For optical spectroscopy, the free-standing Si-QDs were dispersed in UV grade ethanol. More details on production and material characteristics can be found in Ref. [22].

Absorbance, Photoluminescence Spectra, and Lifetime: PL spectra and absorbance in Figure 2 is measured using a thermoelectric-cooled charge coupled device (CCD) detector (Hamamatsu) coupled to an imaging spectrometer (M266, Solar Laser Systems). For excitation a Xe-lamp (150 W, Hamamatsu) (Figure 2b) and a nanosecond-pulsed laser (optical parameter oscillator (OPO) system pumped by Nd:YAG (yttrium aluminum garnet), 7 ns pulse duration, repetition rate 100 Hz) (Figure 2a) are used. The PL lifetime is measured using femtosecond laser pulsed excitation (Ti-sapphire laser pumped optical parameter amplifier (OPA), 140 fs pulse duration, repetition rate of 4 MHz). Signal is detected by a photomultiplier tube (PMT) (Hamamatsu) in a single

photon-counting regime (instrumental response time of 26 ps). All measurements are done at room temperature and are corrected for spectral sensitivity of the detection systems.

Single-QD Photoluminescence Spectra: Single Si-QD PL spectra were measured in wide-field microscopy regime (Figure 3a) by a custom-made set-up based on an inverted microscope (Olympus IX-71) coupled to an imaging spectrograph (Acton SpectraPro 2300i) with a back-thinned CCD camera (Princeton Instruments Spec-10:400B). Highly diluted colloidal suspensions of Si-QDs were drop-casted onto a quartz substrate and placed in the sample compartment. A single objective lens (100 \times , numerical aperture (NA) = 0.8 with working distance of 3–6 mm) was used to focus the excitation light as well as to collect and image the emitted PL in an epi-fluorescence configuration. Excitation by the 405 nm diode laser is sent to the sample through an optical system which enabled excitation of $\sim 36 \mu\text{m}$ spot. The excitation power density is variable between 0.03 and 80 W/cm^2 using neutral density filters. All spectra were corrected for the spectral response of the apparatus and cleared from hot-spots.

Single-QD Photoluminescence Lifetime: The PL lifetime of individual QDs was measured in a confocal regime (Figure 3a) using inverted confocal microscope system (MicroTime 200, PicoQuant). For excitation we used picosecond-pulsed diode laser at 405 nm (LDH-D-C-400B, PicoQuant, 40 MHz repetition rate). The excitation light was focused by the water immersion objective (60 \times /NA = 1.2, Olympus) to the diffraction-limited spot. Light from the nonfocal planes was cut off by 50 μm pinhole placed in the detection plane. Eventually, signal was detected by a single photon avalanche diode (SPAD) (SPCM-AQR-14, PerkinElmer) with instrumental response time of ~ 600 ps.

Supporting Information

Supporting Information is available from the Wiley Online Library or from the author.

Acknowledgements

K.D. and T.G. acknowledge the Dutch Stichting voor Fundamenteel Onderzoek der Materie (FOM) for financial support. Part of this work (C.P.U., J.M.J.P., H.Z.) was funded by the Dutch Polymer Institute (Functional Polymer Systems project no. 681) and (A.F., J.V.) by Charles University through PRVOUK P45 and EC (FP7/2007-2013) under grant agreement n^o: 245977. J.H. and M.H. thank the Czech Science Foundation (via project P208/12/G016). Additionally M.H. acknowledges the Praemium Academie Award (Academy of Sciences of the Czech Republic). The authors thank L. Ruizendaal for assistance with sample preparation, A. N. Poddubny for fruitful discussions, and H. Zhang for assistance with ultrafast spectroscopy. The photograph in Figure 2a was taken by M. T. Trinh.

[1] M. S. Hybertsen, *Phys. Rev. Lett.* **1994**, *72*, 1514.

[2] M. V. Wolkov, J. Jorne, P. M. Fauchet, G. Allan, C. Delerue, *Phys. Rev. Lett.* **1999**, *82*, 197.

- [3] I. Vasiliev, J. R. Chelikowsky, R. M. Martin, *Phys. Rev. B* **2002**, *65*, 121302.
- [4] V. A. Belyakov, V. A. Burdov, R. Lockwood, A. Meldrum, *Adv. Opt. Technol.* **2008**, *2008*, 279502.
- [5] D. Jurbergs, E. Rogojina, L. Mangolini, U. Kortshagen, *Appl. Phys. Lett.* **2006**, *88*, 233116.
- [6] F. Hua, F. Erogbogbo, M. T. Swihart, E. Ruckenstein, *Langmuir* **2006**, *22*, 4363.
- [7] A. Gupta, T. Swihart, H. Wiggers, *Adv. Funct. Mater.* **2009**, *19*, 696–703.
- [8] Z. C. Holman, U. R. Kortshagen, *J. Phys. D* **2011**, *44*, 174009.
- [9] J. D. Holmes, K. J. Ziegler, R. C. Doty, L. E. Pell, K. P. Johnston, B. A. Korgel, *J. Am. Chem. Soc.* **2001**, *123*, 3743–3748.
- [10] D. S. English, L. E. Pell, Z. Yu, P. F. Barbara, B. A. Korgel, *Nano Lett.* **2002**, *2*, 681–685.
- [11] Z. Ding, B. M. Quinn, S. K. Haram, L. E. Pell, B. A. Korgel, A. J. Bard, *Science* **2002**, *296*, 1293.
- [12] J. P. Wilcoxon, G. A. Samara, P. N. Provencio, *Phys. Rev. B* **1999**, *60*, 2704.
- [13] R. D. Tilley, J. H. Warner, K. Yamamoto, I. Matsui, H. Fujimori, *Chem. Commun.* **2005**, *14*, 1833–1835.
- [14] J. H. Warner, A. Hoshino, K. Yamamoto, R. D. Tilley, *Angew. Chem. Int. Ed.* **2005**, *44*, 4550–4554.
- [15] M. Rosso-Vasic, E. Spruijt, B. van Lagen, L. De Cola, H. Zuilhof, *Small* **2008**, *4*, 1835–1841.
- [16] M. Rosso-Vasic, E. Spruijt, Z. Popovic, K. Overgaag, B. van Lagen, B. Grandidier, D. Vanmaekelbergh, D. Domínguez-Gutiérrez, L. De Cola, H. Zuilhof, *J. Mater. Chem.* **2009**, *19*, 5926–5933.
- [17] J. R. Heath, *Science* **1992**, *258*, 1131–1133.
- [18] C.-S. Yang, R. A. Bley, S. M. Kauzlarich, H. W. H. Lee, G. R. Delgado, *J. Am. Chem. Soc.* **1999**, *121*, 5191–5195.
- [19] J. Zou, R. K. Baldwin, K. A. Pettigrew, S. M. Kauzlarich, *Nano Lett.* **2004**, *4*, 1181–1186.
- [20] A. Tanaka, R. Saito, T. Kamikake, M. Imamura, H. Yasuda, *Eur. Phys. J. D* **2007**, *43*, 229–232.
- [21] J. Choi, N. S. Wang, V. Reipa, *Langmuir* **2009**, *25*, 7097–7102.
- [22] L. Ruizendaal, S. P. Pujari, V. Gevaerts, J. M. J. Paulusse, H. Zuilhof, *Chem. Asian J.* **2011**, *6*, 2776–2786.
- [23] L. Ruizendaal, S. Bhattacharjee, K. Pournazari, M. Rosso-Vasic, L. H. J. de Haan, G. M. Alink, A. T. M. Marcelis, H. Zuilhof, *Nanotechnology* **2009**, *3*, 339–347.
- [24] S. Bhattacharjee, L. H. J. de Haan, N. M. Evers, X. Jiang, A. T. M. Marcelis, H. Zuilhof, I. M. C. M. Rietjens, G. M. Alink, *Particle Fibre Toxicol.* **2010**, *7*, 1–12.
- [25] J. Zou, S. M. Kauzlarich, *J. Clust. Sci.* **2008**, *19*, 341–355.
- [26] A. Shiohara, S. Hanada, S. Prabakar, K. Fujioka, T. H. Lim, K. Yamamoto, P. T. Northcote, R. D. Tilley, *J. Am. Chem. Soc.* **2009**, *132*, 248–253.
- [27] J. P. Wilcoxon, G. A. Samara, *Appl. Phys. Lett.* **1999**, *74*, 3164–3166.
- [28] M. Rosso-Vasic, E. Spruijt, B. van Lagen, L. De Cola, H. Zuilhof, *Small* **2009**, *5*, 2637.
- [29] S. Takeoka, M. Fujii, S. Hayashi, *Phys. Rev. B* **2000**, *62*, 16820–16825.
- [30] G. Ledoux, J. Gong, F. Huisken, O. Gullois, C. Reynaud, *Appl. Phys. Lett.* **2002**, *80*, 4834–4836.
- [31] K. Kúsová, O. Cibulka, K. Dohnalová, I. Pelant, J. Valenta, A. Fučíková, K. Žídek, J. Lang, J. Englich, P. Matějka, P. Štěpánek, S. Bakardjieva, *ACS Nano* **2010**, *4*, 4495–4504.
- [32] W. D. A. M. de Boer, D. Timmerman, K. Dohnalová, I. N. Yassievich, H. Zhang, W. J. Buma, T. Gregorkiewicz, *Nat. Nanotechnol.* **2010**, *5*, 878–884.
- [33] L. Tsybeskov, J. V. Vandyshev, P. M. Fauchet, *Phys. Rev. B* **1994**, *49*, 7821–7824.
- [34] J. Valenta, A. Fučíková, I. Pelant, K. Kúsová, K. Dohnalová, A. Aleknavičius, O. Cibulka, A. Fojtík, G. Kada, *New J. Phys.* **2008**, *10*, 073022.
- [35] F. A. Reboredo, G. Galli, *J. Phys. Chem. B* **2005**, *109*, 1072–1078.
- [36] M. D. Mason, G. M. Credo, K. D. Weston, S. K. Buratto, *Phys. Rev. Lett.* **1998**, *80*, 5405–5408.
- [37] J. Valenta, A. Fučíková, F. Vácha, F. Adamec, J. Humpolíčková, M. Hof, I. Pelant, K. Kúsová, K. Dohnalová, J. Linnros, *Adv. Funct. Mater.* **2008**, *18*, 2666–2672.
- [38] J. Martin, F. Cichos, F. Huisken, C. von Borczyskowski, *Nano Lett.* **2008**, *8*, 656–660.
- [39] I. Sychugov, R. Juhasz, J. Valenta, M. Zhang, P. Pirouz, J. Linnros, *Appl. Surf. Sci.* **2006**, *252*, 5249–5253.
- [40] J. Valenta, R. Juhasz, J. Linnros, *Appl. Phys. Lett.* **2002**, *80*, 1070.
- [41] A. N. Poddubny, S. V. Goupalov, V. I. Kozub, I. N. Yassievich, *JETP Lett.* **2009**, *90*, 683.
- [42] a) A. N. Poddubny, private communication; b) The proportionality of Huang–Rhys factor for volume vibrations can be recently found in A. S. Moskalenko, J. Berakdar, A. N. Poddubny, A. A. Prokofiev, I. N. Yassievich, S. V. Goupalov, *Phys. Rev. B* **2012**, *85*, 085432.
- [43] A. Sa'ar, Y. Reichman, M. Dovrat, D. Krapf, J. Jedrzejewski, I. Balberg, *Nano Lett.* **2005**, *5*, 2443–2447.
- [44] M. Mahdouani, R. Bourguiga, S. Jaziri, *Physica E* **2008**, *41*, 228–234.

Received: March 2, 2012
Revised: May 7, 2012
Published online: